

# Plasma Dynamics and Charging Characteristics of a Single Nozzle Ion Head

Jun-Chieh Wang and Mark J. Kushner, University of Michigan, Dept. Electrical Engr. and Comp. Sci., Ann Arbor, MI 48109 USA  
Napoleon Leoni, Henryk Birecki and Omer Gila, Hewlett Packard Research Labs, Palo Alto, CA 94304 USA

## Abstract

A high resolution ion print head architecture which utilizes micro-dielectric barrier discharges (mDBD's) has been developed for charging of surfaces in electrophotographic (EP) printing. The mDBDs consist of arrays of micro-plasma devices (10-100  $\mu\text{m}$  diameter) fabricated using MEMS techniques. A radio frequency (rf) voltage waveform biases an electrode which is buried in a dielectric substrate. A third biasing electrode separated by hundreds of microns from the dielectric surface is used to extract electron charges. To aid in the development and improve the performance of ion-head charging systems, a first principles, multi-dimensional computer modeling investigation has been conducted. The dynamics of the plasma and charging of the top surface as a function of rf frequency, voltage waveform and material properties will be discussed, with comparison of our results to experiments.

## Introduction

Electron current extraction from microplasmas is attractive due to its potential application for surface treatment with high spatial resolution. Among all the microplasma configurations, dielectric barrier discharges (DBDs) [1] are becoming a favored device particularly when operating at higher pressures due to their intrinsic stability against arcing.

DBDs are often used for stable, high-pressure and non-thermal plasma sources. The plasma in DBDs is sustained between dielectric covered electrodes. The electrodes are driven with ac voltages of tens of Hz to radio frequency (rf) – MHz. When DBDs are operated in a filamentary mode, upon initiation the plasma propagates across the gap as a streamer. The streamer electrically charges the opposite dielectric surface and removes the local potential drop across the gap. As the gap voltage falls below its self-sustaining value, the plasma is then terminated. When the polarity changes on the following half ac cycle, a more intense electron avalanche occurs at the same location due to the higher voltage across the gap from the previously charged dielectrics. The plasma is then re-ignited with each rf cycle. Micro-dielectric barrier discharges (mDBDs) are a variant of DBDs where, through use of MEMS technology, the plasma filaments in micro-scale DBDs can be spatially and temporally well controlled. In certain applications such as area selective micrometer surface treatment [2], a third electrode [3,4] can be used to extract electron current out of the mDBDs. As such, mDBDs can be used as sources of charge in ionographic printing.

mDBDs operated at atmospheric pressure have been developed to generate electron current sources for uniformly charging or patterning dielectric surfaces. In this application, an electron current beam tens of microns in diameter is extracted out of a mDBD cavity. Although arrays of these mDBD devices can be used to charge large areas, we will focus our attention in this paper on the operating characteristics of a single mDBD. A

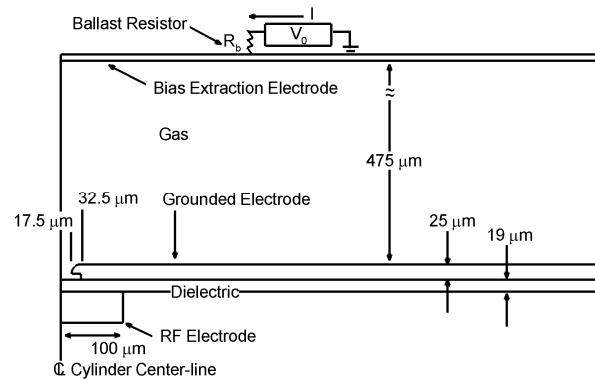


Figure 1. Schematic of a typical single nozzle ion head.

schematic of a single nozzle ion head is shown in Fig. 1. The device consists of a cylindrical micro-cavity 65  $\mu\text{m}$  in diameter in a grounded electrode, separated from an rf powered electrode by a dielectric sheet 15-20  $\mu\text{m}$  thick having a relative permittivity  $\epsilon_r$  up to 20. The rf electrode is buried in a printed-circuit-board. The positively biased current extraction electrode is separated from the mDBD cavity by 400-500  $\mu\text{m}$ .

In this paper we discuss results from a computational investigation of this single nozzle ion head using a mDBD configuration. The model used in this investigation, *nonPDPSIM*, is a first principles, two-dimensional multi-fluid hydrodynamics simulation performed on an unstructured mesh [5]. *nonPDPSIM* solves transport equations for charged and neutral species, Poisson's equation for the electric potential and the electron energy conservation equation for the electron temperature. A Monte Carlo simulation is used to track sheath accelerated secondary electrons emitted from surfaces. Rate coefficients and transport coefficients for the bulk plasma are obtained from local solutions of Boltzmann's equation for the electron energy distribution. Radiation transport is addressed using a Green's function approach.

## Plasma Dynamics and Current Extraction

The plasma dynamics in the mDBD cavity and current extraction to the extraction electrode will first be discussed. The operating conditions are 1 atm of  $\text{N}_2$  with 0.01% of  $\text{O}_2$  as an impurity at 300 K. The rf electrode is biased with 1.4 kV ac at 25 MHz. The top extraction electrode is biased with a 2 kV dc. The time evolution of  $E/N$  (electric field/gas number density) and electron density in the mDBD cavity are shown in Fig. 2 over a single cycle. The electron density in the plume of extracted electron current is shown in Fig. 3. During the negative cycle of

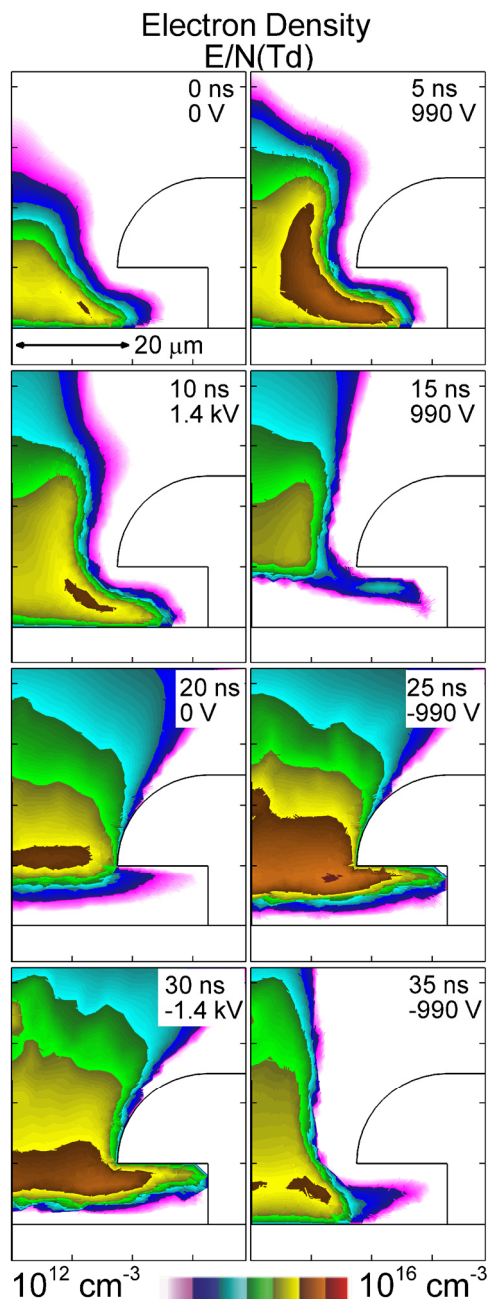


**Figure 2.** Time evolution of electron density (log scale,  $\text{cm}^{-3}$ ) and  $E/N$  [contour labels in Td ( $10^{-17} \text{ V}\cdot\text{cm}^2$ )] in the mDBD cavity at different phases of rf driving voltage of 1.4 kV during a 40 ns (25 MHz) cycle.

the applied rf voltage, the positive ions in the mDBD cavity drift towards the dielectric and charge it positively. When the rf potential ( $V_{rf}$ ) crosses from negative to positive at the beginning of the cycle ( $t = 0$  ns in the figures), the electric field produced by the net voltage in the gap between the top biased electrode and the positively charged dielectric is insufficient for electron current extraction. The electrons in the mDBD drift towards the dielectric and begin to neutralize the positively charged surface. Before the positive peak of  $V_{rf}$  at  $t = 10$  ns, the negative charge collected on

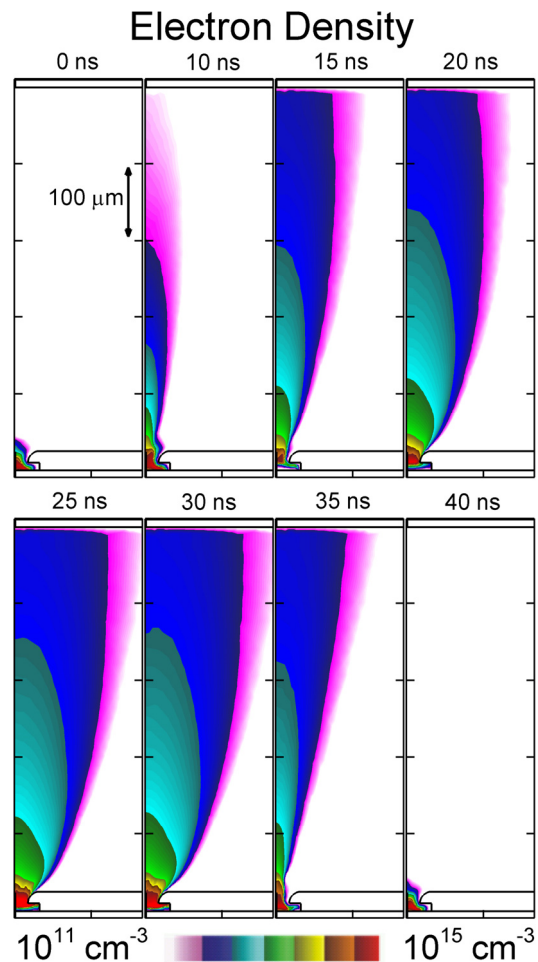


**Figure 3.** Electron plume density (log scale,  $\text{cm}^{-3}$ ) in the gap at different phases of the rf driving voltage of 1.4 kV during a 40 ns (25 MHz) cycle.

the dielectric has neutralized a sufficient amount of the positive charge that there is a net extracting field that accelerates the electron plume out of the mDBD cavity. A small flux of electrons, the prepulse, escapes from the cavity and is accelerated towards the top extraction electrode. This prepulse is magnified with large values of  $dV/dt$  hence is more prominent at higher rf frequencies.

When  $V_{rf}$  decreases to zero at  $t = 20$  ns, a negative potential still exists on the dielectric due to the previous collection of negative charges. At this point, the electric field at the opening to the mDBD cavity extracts the electron plume from the cavity, which then reduces the electron density in the mDBD cavity. At the same time, electron ionization sources in the cavity reach their maximum values ( $10^{25} \text{ cm}^{-3}\text{s}^{-1}$ ) due to avalanching of the remaining residual electrons in the mDBD cavity and by secondary electrons emitted from surfaces in the cavity. This avalanche then enhances the current extraction to the top biased electrode. The electron plume reaches its greatest extent at 30 ns at the negative peak of  $V_{rf}$ . As this proceeds, positive ions are being collected on the dielectric, which reduces the voltage drop across the gap. The electron plume then begins to diminish and nearly extinguishes. The cycle then restarts.

### Current Collection: Frequency Effect

Current collection on the top extraction electrode is sensitive to the rf driving frequency and extraction voltage. Extracted conduction current on the top electrode is shown in Fig. 4 for rf frequencies of 2.5 to 25 MHz. Experiment measurement of electron current at 2.5 MHz with lower extraction voltage (and so lower current) is shown in Fig. 5 for comparison. At 25 MHz, a pre-pulse electron current of 0.3 mA is collected on the top biased electrode and is

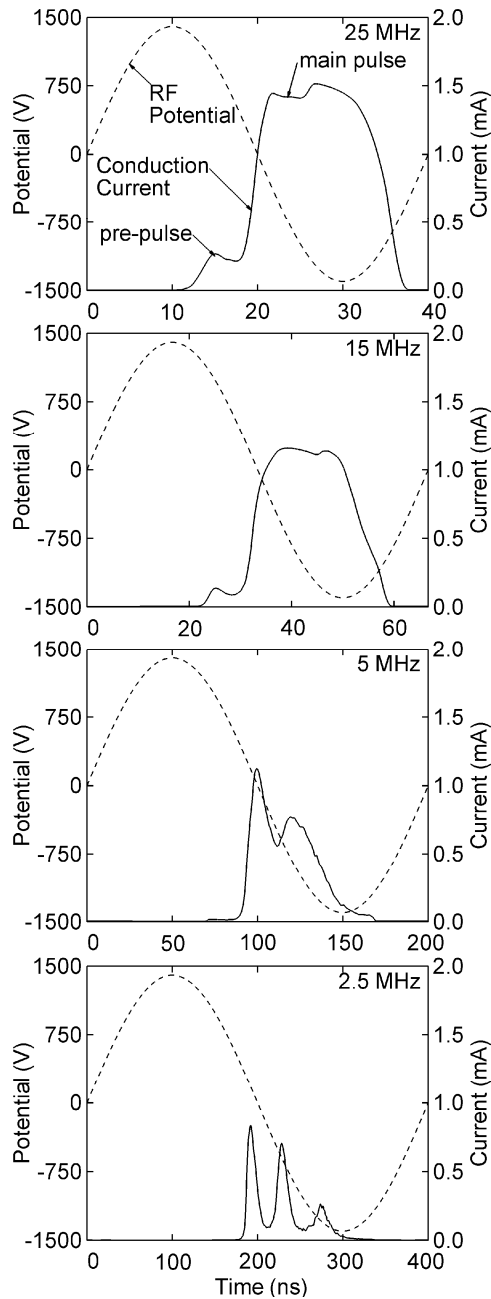


**Figure 4.** rf potential (dash line, volts) and collected current (solid line, mA) for  $V_{rf}=1.4$  kV and extraction voltage of 2 kV. rf frequency ranges from 2.5 to 25 MHz.

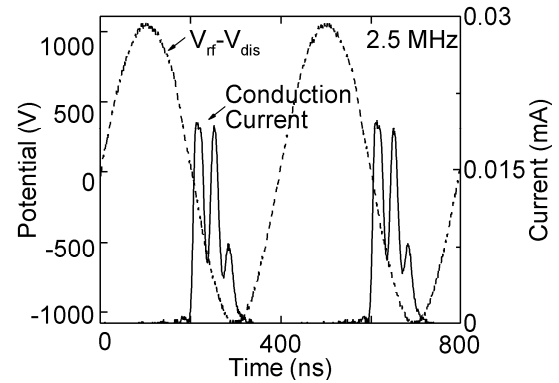


**Figure 5.** Experimentally observed triple current pulsed obtained at 2.5 MHz in the same sandwich mDBD device for equivalent biasing as in the simulation.

followed by a larger main current pulse. At 15 MHz, the pre-pulse is reduced to 0.1 mA due to the smaller  $dV/dt$ . Note that the main current also has greater peak value at higher frequencies as a consequence of this high  $dV/dt$ . At 5 and 2.5 MHz, the pre-pulse current is suppressed, and the main current breaks into multiple current pulses.

The multiple peaks in extracted current driven at lower frequencies are a consequence of periodic bursts of ionization in the mDBD cavity. As mentioned, when  $V_{rf}$  changes its polarity from positive to negative voltage, a negative potential exists on the dielectric due to the previous collection of negative charges. The electron plume is accelerated toward the top biased extraction electrode which reduces the electron density in the mDBD cavity. As the frequency decreases and the rf period becomes longer, there is sufficient electron current extracted to deplete the cavity. The local electric field then rebounds and produces ionization. The electron density is then repopulated in the cavity which enables another burst of electron current to be collected. If  $V_{rf}$  has not yet changed sign, the process can repeat itself. As a result, the main current breaks into multiple current pulses at lower frequencies (5-2.5 MHz).

The multiple pulses of current at 2.5 MHz are experimentally observed when using a similar sandwich mDBD device operated under similar conditions. The experimental voltage drop between the rf and discharge electrode and current collection on the top electrode are shown in Fig. 5. In the experiment, the top extraction electrode is grounded, a -1 kV dc bias is applied to both the rf and discharge electrode, while the rf electrode is also biased with 1 kV ac voltage at 2.5 MHz. (This biasing is electrically equivalent to what was used in the model.) The results from the simulation (shown in Fig. 4, 2.5 MHz) are in basic agreement with the experiment data. The smaller current in the experiment which can be attributed to the smaller rf and extraction voltage, and capacitance of the dielectric sheet. The predicted triple current pulses extracted at the zero crossing of the rf voltage are corroborated by the experiment.

### Total Charge Collection

Time integrated charge collection on the top electrode as a function of time for different rf frequencies, rf voltage and permittivity of the dielectric are shown in Fig. 6. By increasing the

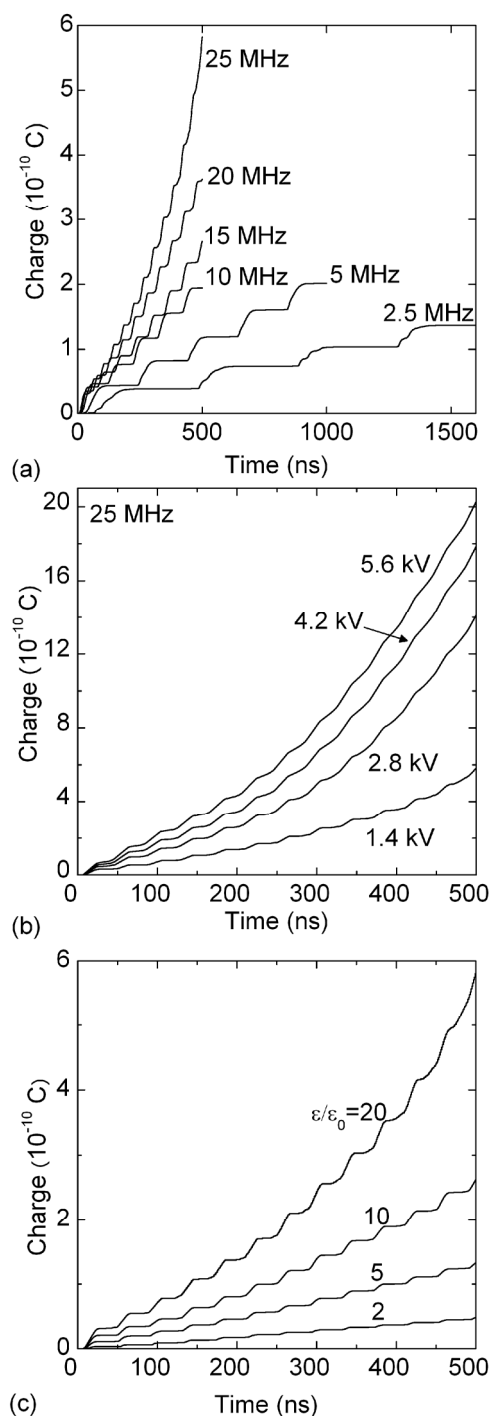


**Figure 6.** Time integrated charge collection on the top 2 kV biased electrode. a) rf frequencies of 25 to 2.5 MHz. b)  $V_{rf}=1.4, 2.8, 4.2$  and 5.6 kV. c)  $\epsilon/\epsilon_0=20, 10, 5$  and 2.

rf driving frequency, charge collection increases due to the higher repetition rate. At lower frequencies, charge collection is limited by capacitance of the dielectric layer above the rf electrode, while at higher frequencies, charge collection is limited by the shorter rf period. The end result is that the charge/pulse is not that different. Integrated charge collection also increase with rf driving voltage.

In general, a higher electron density in the cavity is produced due to the larger  $E/N$  and ionization rate from bulk plasma and sheath accelerated secondary electron ionization. Charge collection increases nearly linearly with  $\epsilon_r$ . Since the intervening dielectric acts as a capacitor whose capacitance scales with  $\epsilon_r$ , its charging characteristics and time integrated charge collection on the top electrode scales with  $\epsilon_r$ .

## References

- [1] U. Kogelschatz, "Dielectric-barrier discharges: Their history, discharge physics, and industrial applications," *Plasma Chem. Plasma Process.* 23, 1 (2003).
- [2] N. Lucas, A. Hinze, C.-P. Klages, S. Büttgenbach, "Design and Optimization of Dielectric Barrier Discharge Microplasma Stamps", *J. Phys. D* 41, 194012 (2008).
- [3] G. Bauville, B. Lacour, L. Magne, V. Puech, J. P. Boeuf, E. Munoz-Serrano, and L. C. Pitchford, "Singlet oxygen production in a microcathode sustained discharge," *Appl. Phys. Lett.*, 90, 031501 (2007).
- [4] S. Muller, R.-J. Zahn, J. Grundmann, "Extraction of Ions from Dielectric Barrier Discharge Configurations", *Plasma Process. Polym.* 4, S1004 (2007).
- [5] Z. Xiong and M. J. Kushner "Surface Corona-Bar Discharges for Production of Pre-ionizing UV Light for Pulsed High Pressure Plasmas", *J. Phys D* 43, 505204 (2010).

## Author Biographies

*Jun-Chieh Wang is a PhD student in the Department of Electrical Engineering and Computer Science at the University of Michigan (UM). He received his B.A. and M.S. in physics from National Cheng Kung University in 2005. Before UM, he worked on fusion plasma theory and ionosphere plasma phenomenon. His current research focuses on low-temperature plasma technology and fundamental plasma physics.*

*Mark J. Kushner received the B.A. & B.S. from the University of California at Los Angeles, and the M.S. & Ph.D. in Applied Physics from the California Institute of Technology. He is a professor in the Electrical Engineering and Compute Science Department at the University of Michigan where he directs the Michigan Institute for Plasma Science and Engineering and the DOE Center for Control of Plasma Kinetics. Prof. Kushner has published more than 270 journal articles on topics related to low temperature plasmas and materials processing. He was recently elected to the National Academy of Engineering.*

*Napoleon Leoni is a Mechanical Engineer in the Commercial Print Engine Lab of Hewlett Packard Laboratories. He received his B.Sc. in Mechanical Engineering from Universidad Simon Bolivar in Venezuela in 1994 and his Ph.D. from Carnegie Mellon University in 1999. Prior to joining HP he worked on the development of nano-positioning systems for disk drive head testers. He joined HP in 2003 and has been working on developing novel charging systems for high speed digital presses.*

*Henryk Birecki is a Senior Scientist at Hewlett Packard Laboratories. He received PhD in physics from the Massachusetts Institute of Technology in 1976 and joined HP Labs in 1978. While at HP he has worked on displays, optical computing, optical recording and other mass storage technologies. He managed projects on optical recording materials and devices and organized international conferences on the subject. Since 2006 he has been working on printing technologies.*

*Omer Gila is managing the "Printing Processes for Digital Commercial Print" department in HP Labs Palo Alto California. Prior to HP Labs, Omer held the positions of COO of Oniyah PSP in Israel and the color control manager in Indigo Rehovot. He holds a B.Sc. (1989) in Physics and Mathematics from the Hebrew University (Jerusalem, Israel) and M.Sc. (1992) in Applied Physics and Electro-optics from the Weizmann Institute of Science (Rehovot, Israel) with honors in both.*